

# Investigating heat shock protein dysregulation and immune cell dynamics in non-alcoholic steatohepatitis by integrated multi-RNA seq analysis

Andrew Dong

Aragon High School, San Mateo, California, USA, 94404.

KEYWORDS. Liver, NASH, RNA-seq, heat shock protein

BRIEF. This study identifies heat shock protein dysregulation and changes in immune cell composition in NASH through RNA-seq analysis of multiple datasets.

---

**ABSTRACT.** The development of non-alcoholic steatohepatitis (NASH) imposes various stresses on hepatocytes due to fatty acid accumulation. Heat shock proteins (HSPs), which play a key role in alleviating these stresses, are important markers in the pathogenesis of NASH. By analyzing multiple RNA-seq datasets from humans and mice, this study identified dysregulation of HSP families, such as HSP70s and HSP90s, in NASH patients. Notably, a significant shift in immune cell populations from macrophages to monocytes was observed during the development of NASH. Among the macrophages in mice liver cells, two distinct groups were identified, namely monocyte-derived macrophages (MDMs) and resident Kupffer cells, with an increase in the proportion of MDMs in NASH. An upregulation of HSPs was also detected in both monocytes and macrophages in NASH. These results reveal the pathogenic role of immune cells in the development of NASH and the critical role of HSPs in responding to these stresses.

---

## INTRODUCTION.

Non-alcoholic steatohepatitis (NASH) is a severe form of non-alcoholic fatty liver disease (NAFLD) characterized by inflammation and liver cell damage due to fat buildup. Affecting 3-6% of Americans, NASH is a progressive condition that can cause liver fibrosis, cirrhosis, and, ultimately, liver failure [1]. Despite its prevalence, NASH remains difficult to diagnose and treat due to symptomatic overlap with less severe forms of liver disease and complex underlying molecular mechanisms that are not yet fully understood [2]. There remains a significant need for deeper investigations into the genetic and cellular factors involved in NASH development, and for the identification of reliable biomarkers that may improve early diagnosis and treatment strategies. NAFLD is defined by the presence of hepatic fat in more than 5% of liver cells in individuals who consume little to no alcohol [3]. Excess carbohydrates are converted via lipogenesis into fatty acids. As these free fatty acids (FFAs) build up, they can overwhelm liver metabolism, creating three major stresses on hepatocytes, including oxidative stress, endoplasmic reticulum (ER) stress, and inflammation [3].

When cells are under stress, the composition of proteins that they produce changes. One of these changes is the increased production of heat shock proteins (HSPs). HSPs are a family of proteins that assist in cellular adaptation to stressors, such as heat, cold, UV light, and tissue injury [4]. In stressed environments, cells rely on HSPs to refold proteins into their functional shapes. For example, HSPs play a role in the response of unfolded proteins to ER stress by directing the formation of critical bonds in these proteins in order to fold them into their appropriate structures. HSPs also contribute to the pathway to degrade misfolded proteins through proteasomes. Finally, when lysosomal proteasomes are overwhelmed with misfolded proteins, HSPs help degrade the aggregation of misfolded proteins to prevent further cell damage [5]. In NASH, HSPs are essential for cellular defense in the liver, although overreaction of HSPs may lead to cell death.

While hepatocytes dominate liver cell populations, immune cells play a crucial role in the progression of NASH [6]. In a healthy liver, different types of immune cells, including Kupffer cells, monocytes, mast cells, and neutrophils, work together to prevent infection and pathogen damage. Kupffer cells are macrophages residing in the liver. They make up 30-35% of all liver cells and account for 95% of all macrophages in the mammalian body [7]. In a healthy liver, Kupffer cells line the sinusoidal capillaries in the liver endothelium, preventing pathogens and their toxic by-products from entering systemic circulation. Kupffer cells initiate an immune response, secreting cytokines and chemokines that amplify liver inflammation and recruit other immune cells. When responding to cell injury, monocytes, derived from hematopoietic stem cells in the bone marrow, migrate to the liver through chemotaxis by liver cells [8]. The monocytes differentiate into macrophages after arriving in the liver. These monocyte-derived macrophages express Kupffer cell markers and are difficult to differentiate from residential Kupffer cells. These monocyte-derived macrophages (MDMs) further promote the inflammatory response, inducing fibrosis to repair damaged tissue and removing necrotic tissue [9]. Characterizing gene expression in healthy versus NASH liver cells can lead to breakthroughs in targeted therapies, potentially preventing the disease from advancing to more critical stages.

This study uses computational tools to analyze a variety of genetic datasets produced by experiments on healthy and NASH liver samples. The analysis identifies trends across samples in the sequenced RNA data to better understand the role of HSPs in the development of NASH disease.

## MATERIALS AND METHODS.

*GSE126848.* GSE126848 is a bulk RNA-seq dataset of liver from 14 healthy individuals with normal-weight, 15 patients with NAFL, and 16 patients with NASH [10].

*GSE235024.* Data used in this study were selected from the bulk dataset GSE235024 designed to investigate the response to lysosomal stress of liver macrophage/Kupffer cells induced by cholesterol crystals in livers on normal diets and those with high-fat-diet (HFD)-induced NASH. In GSE235024, the macrophages isolated from normal livers of wild-type mice that were fed a normal diet or HFD for 6 to 10 weeks were treated with cholesterol crystals at a dose of 500 µg/ml for 24 hours. [11].

*GSE247467.* GSE247467 was a peripheral neutrophil bulk RNA-seq data from NASH patients and healthy individuals. In this dataset, 95% neutrophil purity cells were sequenced. There were 5% peripheral blood mononuclear cells that contributed to the sequenced data [12].

*GSE263970.* GSE263970 was a single-cell RNA-seq dataset. CD45.2+Lin (CD90.2, B220, NK1.1, Siglec-F)-CD11b+ liver innate immune cells were isolated and sequenced from normal and HFD-induced NASH livers [13].

**Bulk RNA-seq data analysis.** The bulk datasets were imported to a DGEList in the edgeR package. After filtering, the data was normalized using calcNormFactors function, and principal component analysis (PCA) was performed to visualize and verify the differences between groups. Then, differential expression analysis was performed between the control groups and treatment groups, obtaining logFC, logCPM, and p-values for each gene. The most significant genes were filtered out as gene markers for the disease [14].

**Single-cell RNA-seq (scRNA-seq) data analysis.** The scRNA-seq data was imported as a Seurat object. Quality control, merging, normalization, and data scaling were applied to the Seurat object. Next, PCA and dimension reduction were performed. The cells on the UMAP plot were grouped into clusters with resolution 0.3. After classifying the data into clusters based on location on the UMAP, the cell type for each cluster was annotated by combining manual annotations and machine learning annotations. The differentially expressed gene list between cell types and between the control and treatment groups for the same cell type were generated [15].

## RESULTS.

**Dysregulations of HSPs in NASH livers.** The J domain of DnaJ (DNAJs), also known as heat shock protein 40 (HSP40), interacts with heat-shock protein 70s (HSP70s). DnaJs interact with HSP70s and play a role in regulating the ATPase activity of Hsp70s. HSP40s and HSP70s act as a complex to bind with misfolded proteins to transport the misfolded protein to lysosome for degradation [16]. HSP90s are a group of heat shock proteins whose molecular weight is 90kD. HSP90s can facilitate not only protein folding but also degradation of misfolded protein. There are three types of HSP90s, namely HSP90A, HSP90B, and TRAP, based on their locations: cytosolic, endoplasmic reticulum, and mitochondrial. In human NAFLD and NASH study GSE126848, 16 HSP genes are significantly upregulated in NASH and NAFLD compared with normal (FDR<0.05) (Figure 1 A). In the human NASH study GSE247467, 17 HSP genes are significantly upregulated in NASH compared with normal (FDR<0.05) (Figure 1 B). In mouse cholesterol crystal stimulated liver macrophage study GSE235024, 12 mouse HSP genes are significantly upregulated in cholesterol stimulated macrophages compared with non-cholesterol control macrophages (FDR<0.05) (Figure 1 C). Overall, HSP90AA1, HSP90AB1, and HSPA8 are significantly upregulated in NASH livers, as evidenced by the RNA-seq data from these three human and mouse NASH liver datasets.

**Shifts of myeloid cells in NASH livers.** CD45.2+Lin (CD90.2, B220, NK1.1, SiglecF)-CD11b+ liver innate immune cells from normal and HFD-induced NASH livers were isolated and sequenced. CD16b is a

cell surface marker mostly for myeloid lineage cells, typically expressed on NK cells, neutrophils, mast cells, monocytes/macrophages, or some T cells. In total, 15,393 cells were sequenced. After filtering out the droplets, there were 13,968 cells analyzed. The scRNA-seq data analysis showed that there were four myeloid lineage cells in normal and HFD NASH livers: monocytes, macrophages/Kupffer cells, mast cells, and neutrophils which were all CD16 positive cells. The UMAP showed these four types of myeloid cells in the mouse liver (Figure 2 A) and the distributions of these four types of cells in normal diet liver (Figure 2 B left) and HFD diet liver (Figure 2 B right). Table S1 shows that there were 27.2% monocytes, 57.4% macrophages/Kupffer cells, 12.7% mast cells, and 2.6% neutrophils in CD16+ cells of normal diet mouse liver, and 41.9% monocytes, 28.8% macrophages/Kupffer cells, 21.3% mast cells, 7.9% neutrophils in CD16+ cells of HFD diet mouse liver. The pie graphs show the cell type proportions of CD16+ myeloid cells, with monocytes in the 12 o'clock position. The majority normal diet CD16+ myeloid cells were macrophages/Kupffer cells, followed by monocytes. There was a shift in cell types in the HFD NASH livers, where the majority CD16+ myeloid cells were monocytes, followed by macrophage/Kupffer cells. Additionally, the number of mast cells increased by 70%, and the number of neutrophils increased by 300% in the HFD mouse liver (Table S1).

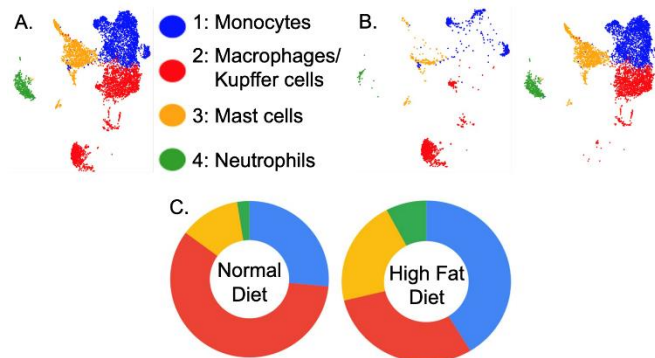


**Figure 2.** Proportions of the sequenced cells from the mouse liver. (A) UMAP shows four types of sequenced cells from mouse liver on a normal diet or HFD. (B) The UMAPs show the distributions of four cell types in the liver of mice on a normal diet (left) or HFD (right). (C) The pie graphs showed the populations of the sequenced cells in the liver of mice on a normal diet or HFD.

**Monocyte subpopulations in HFD-induced NASH liver.** A total of 2535 monocytes from murine livers on a normal diet and HFD were analyzed (Table S1). There were more monocytes in the HFD-induced NASH liver compared with that on a normal diet, 41.9% and 27.2% respectively (Table S1). These monocytes were scattered in the UMAP, which indicated the presence of subclusters (Figure 3 A). UMAP also shows the monocyte distributions in the normal (Figure 3 B) and HFD-induced NASH liver (Figure 3 C).

*Itgam (CD11b)*, *Adgre1 (F4/80)*, *Cd68*, and *Csf1r* are the typical monocyte/macrophage markers and the expressions of these markers by liver monocytes indicate the liver monocyte origin—recruited from the bloodstream monocytes [17]. These monocyte markers were expressed by more monocytes at higher expression levels in the liver of HFD-induced NASH compared with the normal diet (Figure S1 A-D).

The monocytes in the mouse liver also expressed monocyte-recruiting chemokine receptors *Ccr2* and *Cx3cr1* and a lipid receptor *Trem2*. The expression of *Ccr2* and *Cx3cr1* on the liver monocytes indicated that these monocytes recruited other immune cells from the blood through *CCL2-CCR2* and *CX3CL1-CX3CR1* chemotaxis. In the HFD-induced mouse liver, there were not only higher numbers of monocytes expressing *Ccr2* and *Cx3cr1*, but also these monocytes expressed higher levels of *Ccr2* and *Cx3cr1* (Figure S1 F-G).

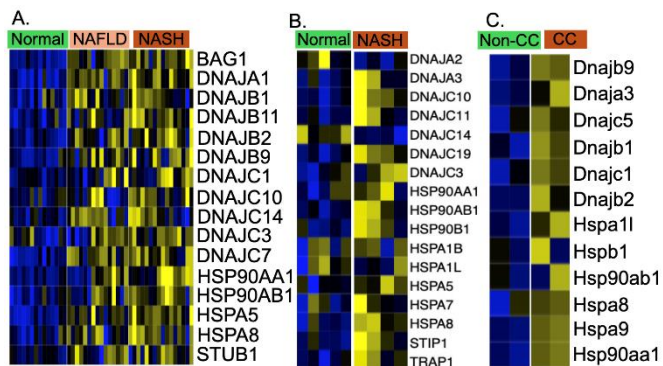


**Figure 1.** Upregulation of HSPs in NASH livers compared with normal livers. (A) GSE126848: 16 HSPs were upregulated in the liver of NASH and NAFLD patients compared with the liver from healthy individuals. (B) GSE247467: 17 HSPs were upregulated in the liver of NASH patients compared with the liver from healthy individuals. (C) GSE235024: 12 HSPs were upregulated in cholesterol crystal stimulated mouse liver macrophages compared with non-cholesterol stimulated controls.

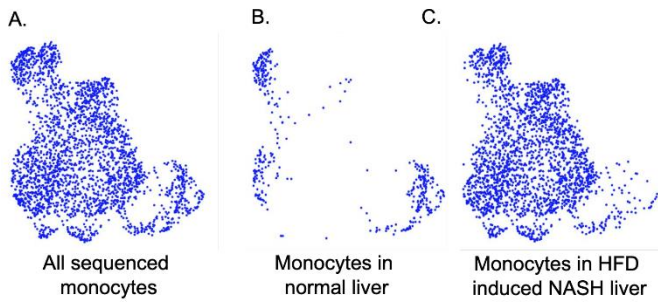


**Figure 3.** The distribution of monocytes in normal and HFD-induced NASH liver. (A) Monocytes in the sequenced cells. (B) The distributions of sequenced monocytes in the normal liver. (C) The distributions of sequenced monocytes in the HFD-induced liver.

*TREM2* is a lipid-binding cell surface receptor that transmits intracellular signals through the adapter *DAP12*. The expression of *Trem2* on liver monocytes helps monocytes handle lipids [18, 19]. The NASH liver monocytes expressed higher levels of *Trem2*, which may play a protective role against lipid overloading (Figure S1 E). But the most outstanding gene expressed in these monocytes is proinflammatory cytokine *Il1b*. The expression of *Il1b* was dramatically increased in both cell number and expression levels in the monocytes of HFD NASH liver compared with normal diet controls (Figure S1 H).

The expression patterns of Hsps were different with the findings from whole liver bulk RNA-seq data analysis (Figure 1). The consistent part was higher expression of *Hsp90aa1* in NASH liver monocytes compared with controls. But there were downregulations of *Hspa8*, *Hsp90ab1*, and *Hsp90b1* (Figure 4). The monocytes lowered the capacity to handle the extra stress by downregulating key HSPs.

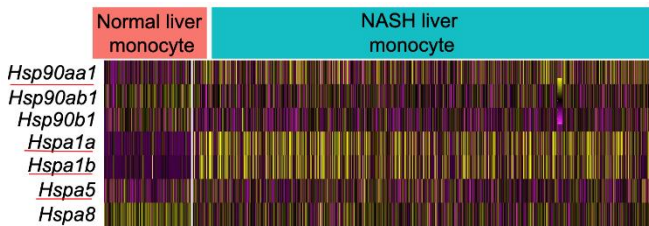


**Figure 4.** Dysregulations of heat shock proteins (HSPs) in the monocytes of HFD-induced NASH liver compared with normal livers. The red underlines marked the significantly upregulated HSPs in the monocyte of NASH liver. The others were the significantly downregulated Hsps.

**Altered macrophages/Kupffer cell population in HFD-induced NASH liver.** A total of 2436 macrophages/Kupffer cells from normal and HFD diet livers were sequenced (Table S1). The 2436 macrophages/Kupffer cells were subclustered into two populations by the cell markers (Table S2) (Figure 5). One cell population majority, shown in normal diet mouse liver and expressing mouse Kupffer cells markers such as *Clec4f*, was named as Kupffer cells (KCs) (Figure 5 A-B). Another major cell population, shown in HFD-induced mouse liver and expressing mouse monocyte/macrophage markers such as *Itgam*, was MDMs (Figure 5 A&C). KCs are the resident long-live macrophages in the liver which are capable of self-renewal. Liver MDMs are short lived cells and are present at low levels during physiologic conditions. The majority of macrophages/Kupffer cells in normal diet liver are KCs and on the other hand, there were more MDMs in HFD-induced mouse NASH liver (Figure 5 B-C).

Although they are all macrophages, the resident macrophage KCs can be distinguished from MDMs based on the cell markers. Markers of KCs included *Clec4f*, *Tim4*, *Vsig4*. In normal livers, KCs expressed high levels of *Clec4f*, *Tim4*, *Vsig4* (Figure S2 A-C). The MDMs expressed very low or no levels of *Clec4f*, *Tim4*, *Vsig4* in both healthy

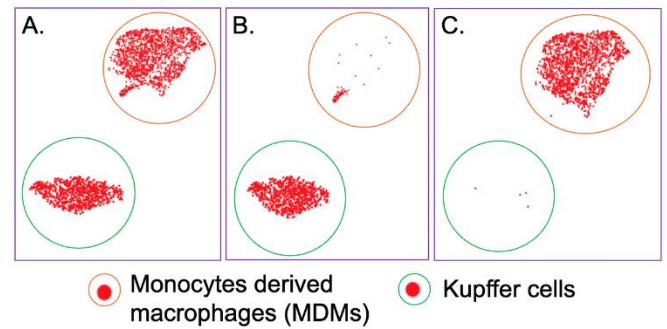


**Figure 5.** Two subtypes of macrophages/Kupffer cells in mouse liver. (A) Two subtypes of macrophages/Kupffer cells in the sequenced cells, namely Kupffer cells (lower, green circled cells) and MDMs (upper, red circled cells). (B) There were increased numbers of KCs in the normal liver. (C) There were increased numbers of MDMs in the HFD-induced NASH liver.

and HFD-induced NASH livers (Figure S2 A-C). Monocyte/macrophage markers such as *Itgam*, *Adgre1*, *CD68*, *Csf1r* were detected in both KCs and MDMs (Figure S2 D-G). In HFD-induced NASH liver, the MDMs cells expressed higher levels of lipid receptor *Trem2* and *CD9* (Figure S2 H&K). In HFD-induced NASH liver, the MDMs cells expressed higher levels of monocyte recruitment chemokine receptor *Ccr2*, *Cx3cr1* (Figure S2 I-J). In HFD-induced NASH liver, the MDMs cells also expressed higher levels of *Il1b*, which also indicates higher levels of inflammation in the HFD-induced NASH liver compared with normal diet controls (Figure S2 L).

There were only five KCs in the HFD-induced NASH group, which were indistinguishable from KCs from normal livers. In this study, the MDMs in both normal and HFD-induced NASH livers were compared. Due to the stress in NASH, the MDMs upregulated the expression of *Hsp90aa1*, *Hsp90a1b*, *Hspa1a*, *Hspa1b* while downregulating the expression of *Hsp90b1*, *Hspa5* and *Hspa8* (Figure S3). Excessive stress leads to degradation processes in overburdened MDMs. The MDMs respond by lowering the key processing HSPs such as *Hsp90b1*, *Hspa5*, and *Hspa8* to maintain the lysosome function, consequently lowering their capacity to handle the extra stress by down-regulating key HSPs.

## DISCUSSION.

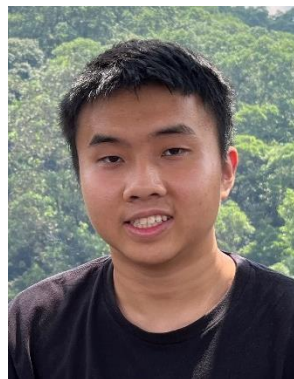
This study analyzed four RNA-seq datasets, including both bulk and scRNA-seq data, to examine the expression profiles of heat shock proteins (HSPs) in the livers of individuals with non-alcoholic steatohepatitis (NASH). In both human and murine bulk RNA-seq data, a consistent upregulation of key HSPs, such as HSPA5, HSPA8, and HSP90 families, was observed in NASH livers. However, in the scRNA-seq analysis of CD11b+ immune cells from an HFD-induced mouse NASH model, HSP expression patterns appeared more complex. While HSP90 family members were upregulated in NASH monocytes and MDMs, key HSPs such as HSPA5 and HSPA8 showed downregulation in these specific immune cell populations. This contrast may stem from the dominant presence of hepatocytes in liver tissue. Hepatocytes may have upregulated HSPA5 and HSPA8 expression to a degree that masked the downregulation observed in CD11b+ immune cells in the bulk RNA-seq data, leading to conflicting results between bulk and single-cell analyses. In the NASH liver, the immune response intensifies, creating a feedback loop of inflammation and liver damage. Kupffer cells, which play a key role in liver immunity, respond to hepatocyte injury by releasing proinflammatory signals, such as IL-1 $\beta$  [7]. Monocytes are then recruited from circulation, where they differentiate into MDMs and actively participate in the inflammatory response [20].

This study revealed distinct patterns of HSP expression in the human NASH liver, with significant upregulation of HSPA5, HSPA8, and HSP90 family proteins. In the HFD-induced mouse NASH model, HSP90 upregulation was also observed in immune cell subtypes, particularly monocytes and MDMs. However, some HSPs, like HSPA5 and HSPA8, were downregulated in these immune cells, underscoring cell-type-specific differences in HSP expression. Additionally, NASH was associated with substantial shifts in immune cell populations, notably a decrease in resident Kupffer cells and an increase in monocytes and MDMs. These findings suggest that HSPs and immune cell shifts may play a dual role in either promoting NASH progression or providing a compensatory response to cellular stress in NASH livers. Understanding these cell-specific dynamics offers insights into the pathogenic mechanisms underlying NASH and may guide the development of targeted therapeutic strategies.

**SUPPORTING INFORMATION.** Supporting information includes a table showing the proportions of immune cells in the healthy and NASH liver samples (Table S1), a table showing the proportion of monocyte-derived macrophages and Kupffer cells within the broader macrophage category (Table S2), two figures showing the gene expression patterns of key HSP genes in monocytes and macrophages (Figure S1 & S2), and a heatmap figure showing the expression levels of HSP genes in healthy and NASH monocyte-derived macrophages (Figure S3).

#### REFERENCES

1. A. C. Sheka, O. Adeyi, J. Thompson, B. Hameed, P. A. Crawford, S. Ikramuddin, Nonalcoholic steatohepatitis: A review. *JAMA* **323**, 1175–1183 (2020).
2. A. M. Oseini, A. J. Sanyal, Therapies in non-alcoholic steatohepatitis (NASH). *Liver Int.* **37**, 97–103 (2017).
3. P. Sahu, P. Chhabra, A. M. Mehendale, A comprehensive review on non-alcoholic fatty liver disease. *Cureus* **15**, e50159 (2023).
4. C. Hu, J. Yang, Z. Qi, H. Wu, B. Wang, F. Zou, H. Mei, J. Liu, W. Wang, Q. Liu, Heat shock proteins: Biological functions, pathological roles, and therapeutic opportunities. *MedComm (2020)* **3**, e161 (2022).
5. J. H. Wolf, T. R. Bhatti, S. Fouraschen, S. Chakravorty, L. Wang, S. Kurian, D. Salomon, K. M. Olthoff, W. W. Hancock, M. H. Levine, Heat shock protein 70 is required for optimal liver regeneration after partial hepatectomy in mice. *Liver Transpl.* **20**, 376–385 (2014).
6. T. Huby, E. L. Gautier, Immune cell-mediated features of non-alcoholic steatohepatitis. *Nat. Rev. Immunol.* **22**, 429–443 (2022).
7. A. Elchaninov, P. Vishnyakova, E. Menyailo, G. Sukhikh, T. Fatkhudinov, An eye on Kupffer cells: Development, phenotype and the macrophage niche. *Int. J. Mol. Sci.* **23**, 9868 (2022).
8. K. Roth, C. E. Rockwell, B. L. Copple, Differential sensitivity of Kupffer cells and hepatic monocyte-derived macrophages to bacterial lipopolysaccharide. *Clin. Exp. Gastroenterol. Hepatol.* **1**, 106 (2019).
9. D. Feng, X. Xiang, Y. Guan, A. Guillot, H. Lu, C. Chang, Y. He, H. Wang, H. Pan, C. Ju, S. P. Colgan, F. Tacke, X. W. Wang, G. Kunos, B. Gao, Monocyte-derived macrophages orchestrate multiple cell-type interactions to repair necrotic liver lesions in disease models. *J. Clin. Invest.* **133**, e166954 (2023).
10. M. P. Suppli, K. T. G. Rigbolt, S. S. Veidal, S. Heebøll, P. L. Eriksen, M. Demant, J. I. Bagger, J. C. Nielsen, D. Oró, S. W. Thrane, A. Lund, C. Strandberg, M. J. Kønig, T. Vilsbøll, N. Vrang, K. L. Thomsen, H. Grønbaek, J. Jelsing, H. H. Hansen, F. K. Knop, Hepatic transcriptome signatures in patients with varying degrees of nonalcoholic fatty liver disease compared with healthy normal-weight individuals. *Am. J. Physiol. Gastrointest. Liver Physiol.* **316**, G462–G472 (2019).
11. M. Itoh, A. Tamura, S. Kanai, M. Tanaka, Y. Kanamori, I. Shirakawa, A. Ito, Y. Oka, I. Hidaka, T. Takami, Y. Honda, M. Maeda, Y. Saito, Y. Murata, T. Matozaki, A. Nakajima, Y. Kataoka, T. Ogi, Y. Ogawa, T. Suganami, Lysosomal cholesterol overload in macrophages promotes liver fibrosis in a mouse model of NASH. *J. Exp. Med.* **220**, e20220681 (2023).
12. A. C. Maretti-Mira, M. P. Salomon, S. Chopra, L. Yuan, L. Golden-Mason, Circulating neutrophil profiles undergo a dynamic shift during metabolic dysfunction-associated steatohepatitis (MASH) progression. *Biomedicine* **12**, 1105 (2024).
13. A. Iwata, J. Maruyama, S. Natsuki, *et al.*, Egr2 drives the differentiation of Ly6C<sup>hi</sup> monocytes into fibrosis-promoting macrophages in metabolic dysfunction-associated steatohepatitis in mice. *Commun. Biol.* **7**, 681 (2024).
14. M. E. Ritchie, B. Phipson, D. Wu, Y. Hu, C. W. Law, W. Shi, G. K. Smyth, *limma* powers differential expression analyses for RNA-seq and microarray studies. *Nucleic Acids Res.* **43**, e47 (2015).
15. M. Su, T. Pan, Q. Z. Chen, W. W. Zhou, Y. Gong, G. Xu, H. Y. Yan, S. Li, Q. Z. Shi, Y. Zhang, X. He, C. J. Jiang, S. C. Fan, X. Li, M. J. Cairns, X. Wang, Y. S. Li, Data analysis guidelines for single-cell RNA-seq in biomedical studies and clinical applications. *Mil. Med. Res.* **9**, 68 (2022).
16. Q. Liu, C. Liang, L. Zhou, Structural and functional analysis of the Hsp70/Hsp40 chaperone system. *Protein Sci.* **29**, 378–390 (2020).
17. S. Daemen, A. Gainullina, G. Kalugotla, L. He, M. M. Chan, J. W. Beals, K. H. Liss, S. Klein, A. E. Feldstein, B. N. Finck, M. N. Artyomov, J. D. Schilling, Dynamic shifts in the composition of resident and recruited macrophages influence tissue remodeling in NASH. *Cell Rep.* **34**, 108626 (2021).
18. D. A. Jaitin, L. Adlung, C. A. Thaiss, A. Weiner, B. Li, H. Descamps, P. Lundgren, C. Bleriot, Z. Liu, A. Deczkowska, H. Keren-Shaul, E. David, N. Zmora, S. M. Eldar, N. Lubezky, O. Shibolet, D. A. Hill, M. A. Lazar, M. Colonna, F. Ginhoux, H. Shapiro, E. Elinav, I. Amit, Lipid-associated macrophages control metabolic homeostasis in a Trem2-dependent manner. *Cell* **178**, 686–698.e14 (2019).
19. V. I. Chandran, C. W. Wernberg, M. M. Lauridsen, M. K. Skytthe, S. M. Bendixen, F. T. Larsen, C. D. Hansen, L. L. Grønkvær, M. S. Siersbæk, T. D. Caterino, S. Detlefsen, H. J. Møller, L. Grøntved, K. Ravnskjaer, S. K. Moestrup, M. S. Thiele, A. Krag, J. H. Graversen, Circulating TREM2 as a noninvasive diagnostic biomarker for NASH in patients with elevated liver stiffness. *Hepatology* **77**, 558–572 (2023).
20. D. Feng, X. Xiang, Y. Guan, A. Guillot, H. Lu, C. Chang, Y. He, H. Wang, H. Pan, C. Ju, S. P. Colgan, F. Tacke, X. W. Wang, G. Kunos, B. Gao, Monocyte-derived macrophages orchestrate multiple cell-type interactions to repair necrotic liver lesions in disease models. *J. Clin. Invest.* **133**, e166954 (2023).



Andrew Dong is a student at Aragon High School in San Mateo, CA.